research report

Experimental Study on System Reliability of Cold-Formed Steel Roof Trusses

Report RP17-1

January 2017

American Iron and Steel Institute

DISCLAIMER

The material contained herein has been developed by researchers based on their research findings and is for general information only. The information in it should not be used without first securing competent advice with respect to its suitability for any given application. The publication of the information is not intended as a representation or warranty on the part of the American Iron and Steel Institute or of any other person named herein, that the information is suitable for any general or particular use or of freedom from infringement of any patent or patents. Anyone making use of the information assumes all liability arising from such use.

UNIVERSITY OF NORTH TEXAS

Experimental Study on System Reliability of Cold-Formed Steel Roof Trusses

Report No. UNT-GP6469

By

Adam Johnson
Research Assistant

Cheng Yu, PhD
Professor

A Research Report Submitted to the American Iron and Steel Institute
January 24, 2017

Department of Engineering Technology
University of North Texas
Denton, Texas 76207

Abstract

This report presents a research project aimed at advancing the treatment of cold-formed steel (CFS) structural reliability in roof trusses. Structural design today relies almost exclusively on component-level design; so, structural safety is assured by limiting the probability of failure of individual components. Reliability of the entire system is typically not assessed, so in a worst-case scenario the system reliability may be less than the component reliability, or in a best-case scenario the system reliability may be much greater than the component reliability. A roof truss itself, is a subsystem with several possible failure modes that are being studied in this test program. These trusses are constructed of CFS members that nest with one another at the truss nodes and are connected by drilling fasteners through the mated surfaces, as well as having steel sheathing fastened to the top chords for lateral bracing. Presented in this paper is a series of full-scale static tests on single as well as systems of CFS roof trusses with a unique experimental setup. The test specimens were carefully monitored to address multiple failure modes: buckling of the top chord, buckling of the truss webs, and any connection failures. This report includes the details of the test program and the experimental results.

Table of Contents

Introduction…….....4
Test Setup…….....4
Test Setup for Truss System……8
Test Specimens…….....9
Test Results…….....10
Truss System Test Results……..18
Conclusion…… .21
Acknowledgements……....22
References……..23
Appendices…….24

Introduction

System reliability is a well-developed topic from a theoretical perspective, however there are still many barriers to its implementation in cold-formed steel (CFS) design. Direct simulations to obtain the system probability of failure while considering strength, material properties, and applied loads as random variables is one possible approach. However, the required statistics are often not available and high reliability computational simulations of a real building to collapse remain elusive, with many of these simulations requiring a Monte Carlo approach. Element based load resistance factor design (LRFD) has served the structural engineering design community well with its conceptual simplicity, but its equivalent for complex structural systems such as buildings or even bridges, or for simpler subsystems such as walls and roofs, are not well developed enough, resulting in the reliability of an element (i.e. a CFS stud member) being misaligned with the reliability of the system (i.e. several studs connected with bridging and sheathing to make a load bearing wall). With that in mind it should be noted that the goal of this research is to advance the treatment of CFS structural reliability in roof trusses and to ultimately move that much closer to a solution to system reliability in their structural design, where this paper will present the results gathered from a series of full scale static tests on single as well as a system of CFS roof trusses with a unique experimental setup.

Test Setup

Test Setup for Single Truss Tests

Trusses are constructed of CFS members that nest with one another at the truss nodes and are connected by self-drilling screw fasteners through the mated surfaces. Steel or wood sheathing is thoroughly fastened to the truss top chords and provide lateral bracing. A roof truss itself, is a subsystem with several possible failure modes that will be studied in this test program. The testing equipment that will be used consists of 12 hydraulic cylinders that can apply a uniform downward pressure to the top chord of the truss. Figures 1 and 2 respectively illustrate the testing setup for single truss specimen manufactured by Aegis and TrusSteel companies. Figure 3 is a photograph taken during our first trial test for the TrusSteel single truss tests.

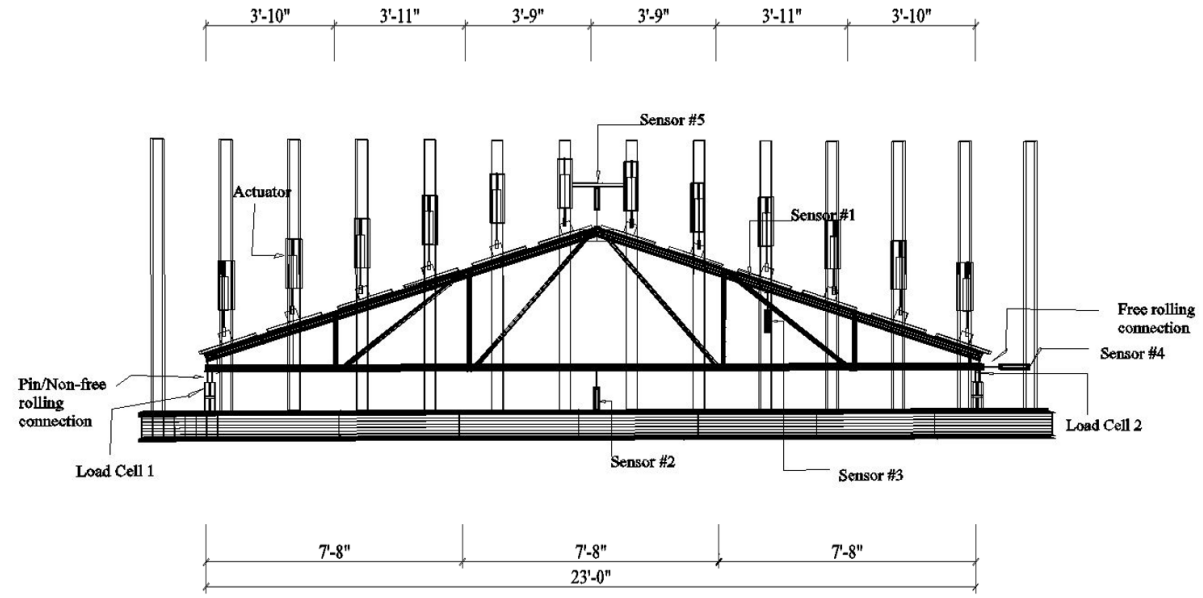

Figure 1: Test Setup for Aegis Single Truss

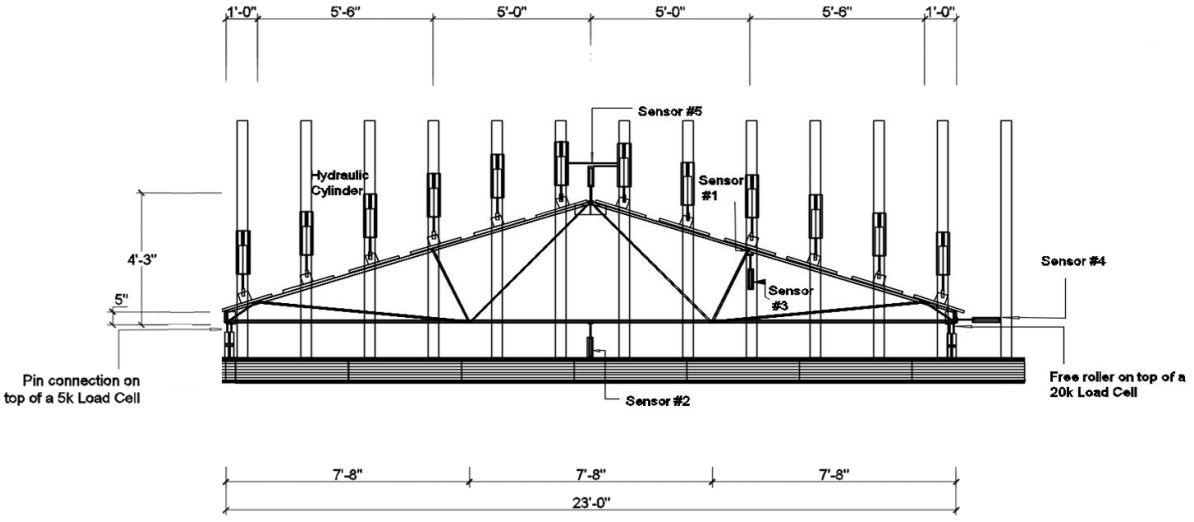

Figure 2: Test Setup for TrusSteel Single Truss

The single truss setup used three sensors to measure the vertical displacement along the top chord and bottom chord. One vertical sensors was located on the bottom chord (sensor #2). Another sensor was placed at the truss' peak (sensor #5) and another was located along the top chord (sensor #3). The fourth sensor was located at the rolling connection of the truss (sensor #4) and used to record the horizontal displacement. The last sensor was located on the top chord (sensor #1) near another sensor but was used to record the out-of-plane displacement of the truss.

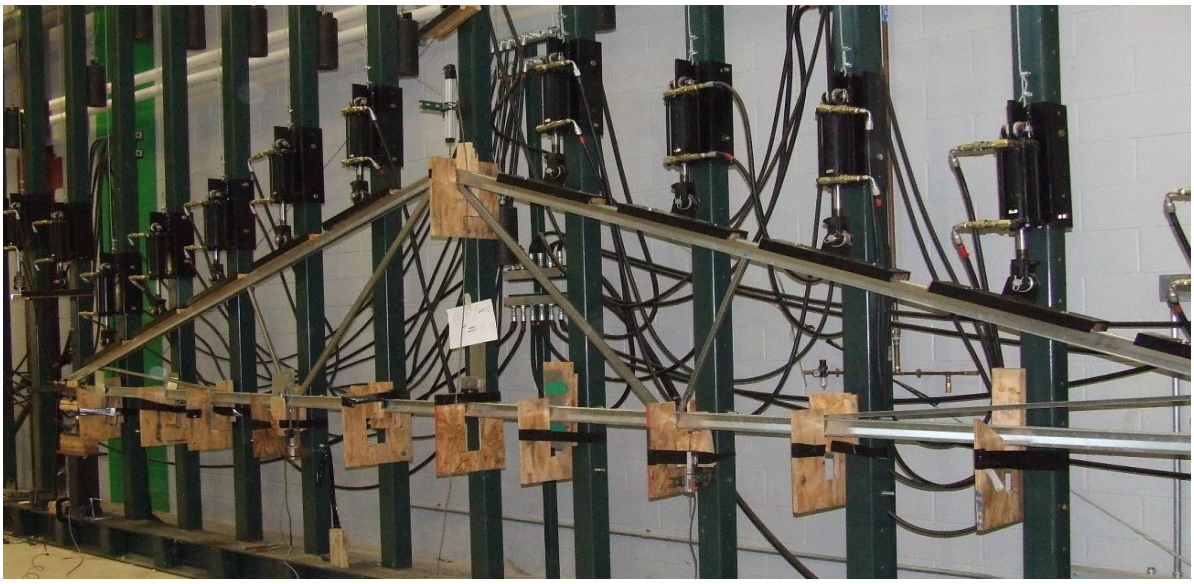

Figure 3: TrusSteel Test Setup

A series of full-scale static tests on CFS roof trusses with a unique experimental setup were conducted in the University of North Texas' structural testing laboratory. The test specimens were carefully monitored and three main failure modes were observed: buckling of the top chord, buckling of the truss webs, and any connection failures. Table 1 lists the testing matrix that was used to test the two different truss profiles in this research and Figure 3 is a photograph taken during our first trial test for the single truss tests.

Table 1: Test Matrix

Truss Profile	System Test	Truss Slope	Truss Span	Force Profile	Test per Profile	Trial Test	Extra Tests
TrusSteel	single truss	4:12	23 ft.	gravity	3	1	1
	2 trusses connected w/ metal b-deck sheathing				3	1	1
Aegis	single truss	4:12	23 ft.	gravity	3	1	1
	2 trusses connected w/ metal b-deck sheathing				3	1	1

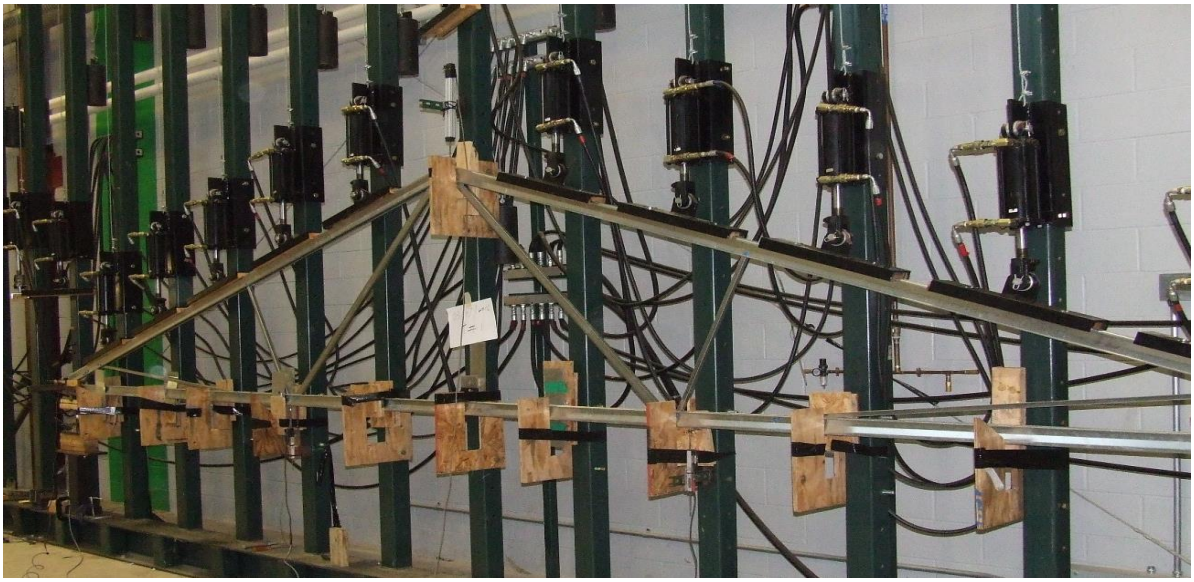

Figure 4: TrusSteel Test Setup

Test Setup for Truss System

In addition to the single truss tests, as specified in the truss testing matrix in Table 1, system tests were also performed using two trusses that were primarily connected using CFS steel corrugated decking. Figure 5 is a photograph taken of the system truss tests.

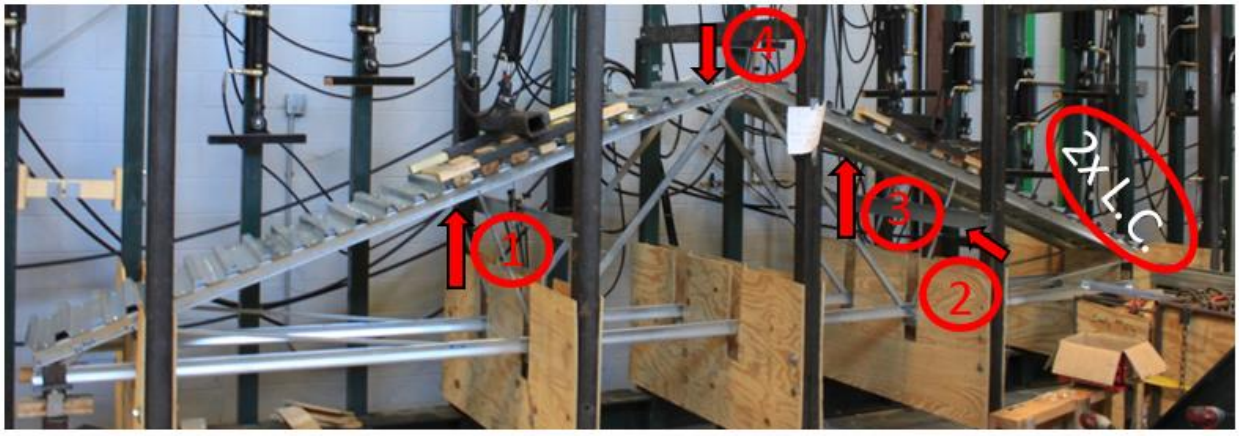

Figure 5: System Truss Setup TrusSteel

Figure 5 shows the test setup for the system tests, as well as how the trusses were braced to limit out-of-plane movement. The system test setup differed from the single truss setup in that it used a different loading pattern. The system trusses used two-point loading systems located at a third of

the length of the trusses, versus the uniformly distributed loading applied to the single trusses. Two sensors were used to measure the displacement of both joints where the top chord, bottom chord, and web members converge (sensors #1 and #3). Another sensor was placed at the peak of the trusses (sensor #4). Finally, the fourth sensor was to be placed on a web member to record the out-of-plane movement for the truss system (sensor #2).

Test Specimens

As indicated in previous section, CFS roof trusses manufactured from two companies, Aegis and TrusSteel. The truss dimension details are provided in the Appendix. To verify the material properties of the trusses as well as ensure the correct data was used for the analysis, coupon tests were performed on each component for each truss configuration. Coupon tests were conducted per the ASTM A370-06 "Standard Test Methods and Definitions for Mechanical Testing of Steel Products". The coupon test results are summarized in Table 2.

The test results indicate that the coupons meet the minimum ductility requirement by North American Specification for Design of Cold-Formed Steel Structural Members 2016 Edition (AISI S100-16), which requires the tensile strength to yield strength ratio greater than 1.08, and the elongation on a 2-in. gage length higher than 10%.

Table 2: Coupon Test Results

Member	Uncoated Thickness (in.)	Yield Stress F_y, (ksi)	Tensile Strength F_u (ksi)	F_u/F_y	Elongation for 2 in. Gage Length (%)
TrusSteel Bottom Chord	0.03512	67.3	81.3	1.207	15.7%
TrusSteel Top Chord	0.03603	67.2	87.0	1.294	31.2%
TrusSteel Web Member	0.03419	65.5	71.4	1.091	25.1%
Aegis Bottom Chord	0.03478	56.7	70.9	1.249	30.6%
Aegis Top Chord	0.03519	55.4	60.3	1.089	26.1%
Aegis Web Member	0.03471	54.7	60.8	1.111	22.6%

Test Results

Single Truss Test Results

This research is investigating the system reliability of the trusses as well as their relationship between the components reliability. The failure sequences, load re-distribution mechanisms, and the load vs. deflection responses at various stages are being studied. The figures below illustrate the test results for two TrusSteel single trusses. The figures show the applied load vs. vertical displacement at the ridge of each truss along with failure mode at each peak point. The first failures for these tests all occurred in their top chords that experienced local buckling. After the top chords failed the web components were the next to fail right before the truss system reached its ultimate capacity.

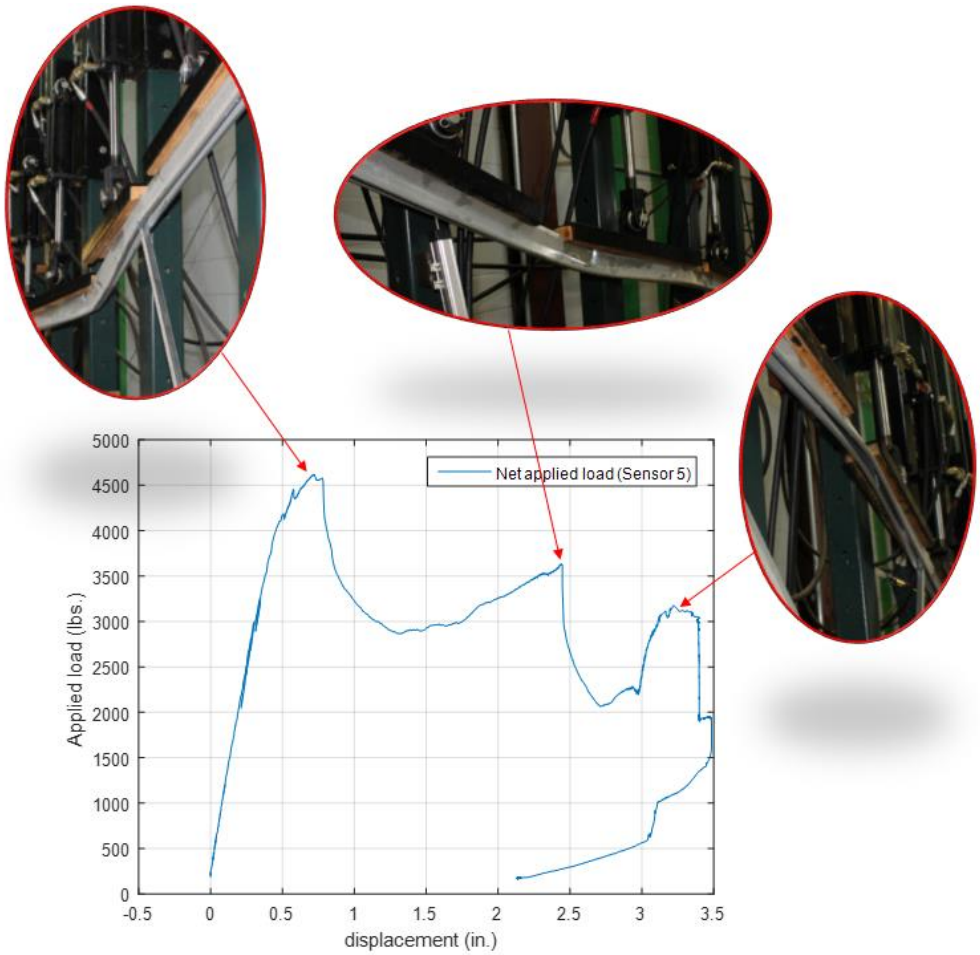

Figure 6: TrusSteel Testing summary of midpoint displacement sensors with failure pictures at peak loads (TrusSteel Test #2)

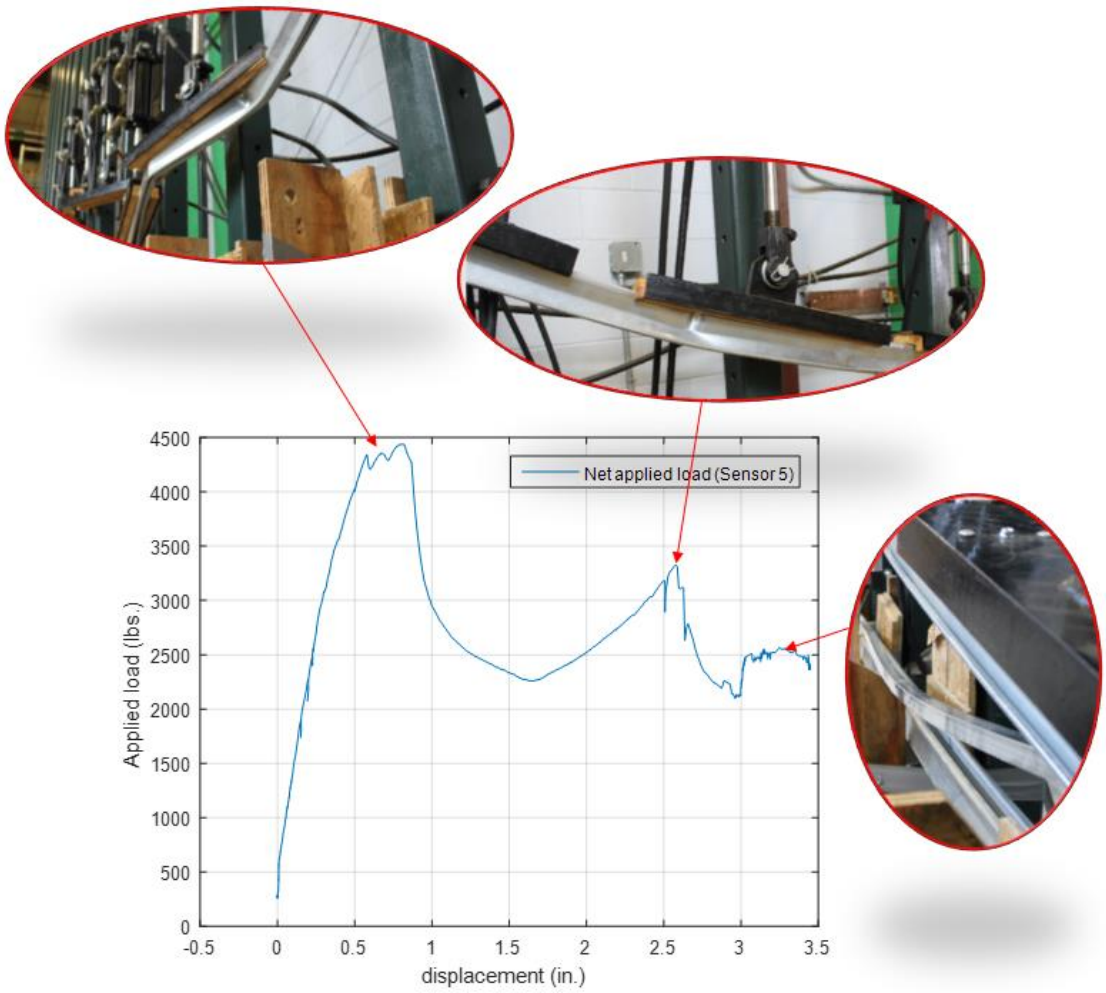

Figure 7: TrusSteel Testing summary of midpoint displacement sensors with failure pictures at peak loads (TrusSteel Test #5)

Figures 6 and 7 illustrate the test results for two TrusSteel single trusses. The figures show the applied load vs. vertical displacement at the ridge of each truss along with failure mode at each peak point. The trusses in these tests both had their first failing component in the top chord. The top chord failed due to local buckling

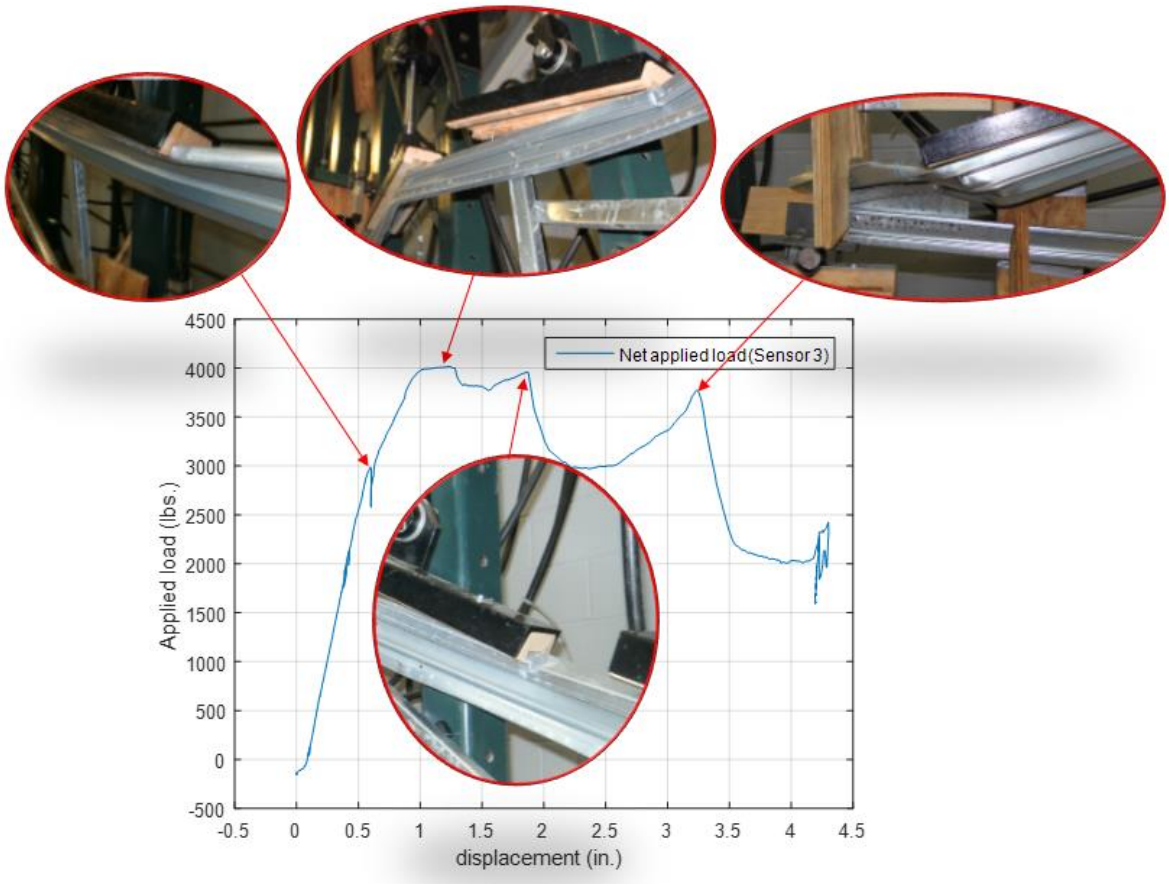

Figure 8: Aegis Testing summary of B.C. midpoint displacement sensors with failure pictures at peak loads (Aegis Test #3)

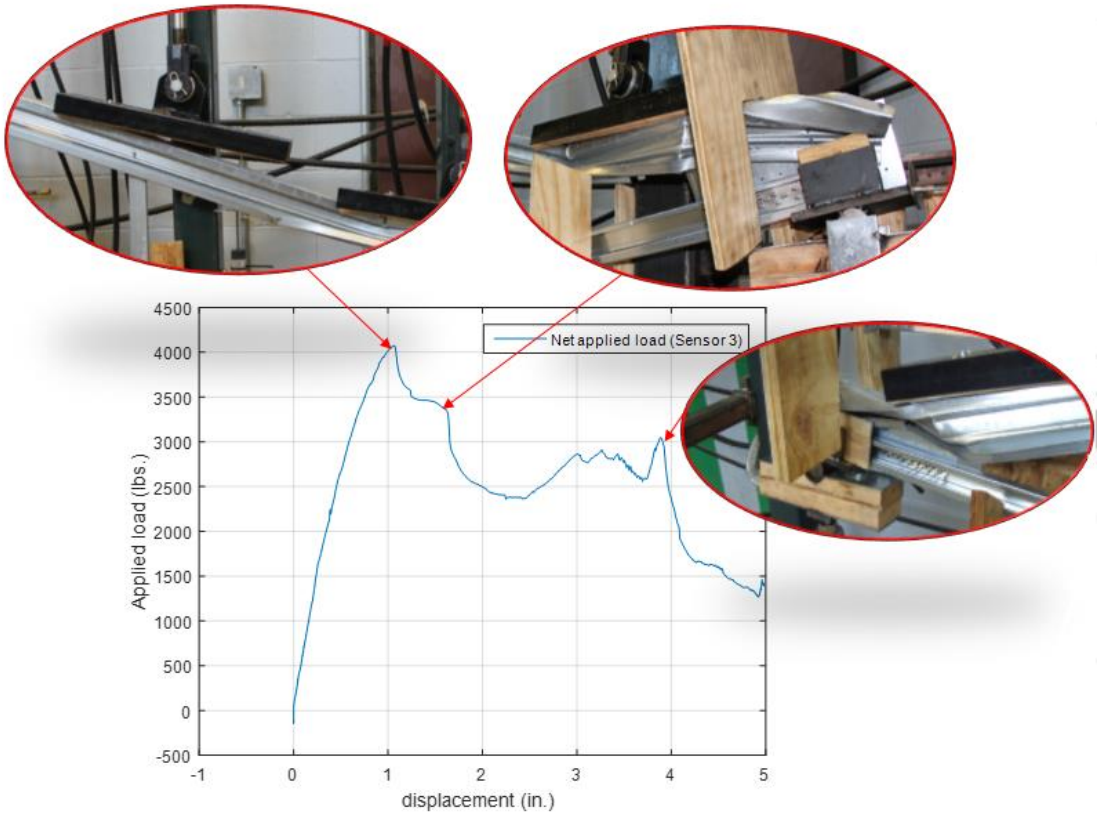

Figure 9: Aegis Testing summary of B.C. midpoint displacement sensors with failure pictures at peak loads (Aegis Test #5)

Figures 8 and 9 illustrate the different failure modes that were recorded using the sensor located at the peak of the truss for two of the truss tests performed for the Aegis configurations. Also, Table 3 lists the observed failure mode sequence for all single truss tests. Table 4 provides the peak loads and associated displacement for single truss tests.

Table 3: Observed Failure Modes for Single Truss Tests

Truss Label	Failure Mode for 1st Peak	Failure Mode for 2nd Peak
TrusSteel Configuration	Top chord failures	Web member failures
Aegis Configuration	Top chord failures	Top chord failures

Table 4: Test Results for Single Truss Tests

Truss Label	1st Peak Load (kips)		Deflection @ 1st Peak (in.)					2nd Peak Load (kips)		Deflection @ 2nd Peak (in.)				
	Load Cell #1	Load Cell #2	Sensor #1	Sensor #2	Sensor #3	Sensor #4	Sensor #5	Load Cell #1	Load Cell #2	Sensor #1	Sensor #2	Sensor #3	Sensor #4	Sensor #5
TrusSteel T#1	2.37	2.69	0.636	0.126	0.052	0.050	0.797	1.93	2.19	0.732	0.075	0.337	0.220	2.58
TrusSteel T#2	2.22	2.60	0.630	0.198	0.012	0.247	0.721	1.74	1.97	0.810	-	0.348	0.387	2.470
TrusSteel T#3	2.26	2.57	0.908	0.087	0.003	0.128	0.942	1.79	2.03	1.120	0.097	0.157	0.221	2.841
TrusSteel T#4	2.10	2.38	0.531	0.236	0.003	0.212	0.809	1.58	1.80	0.792	0.081	0.380	0.418	2.583
Aegis T#1	1.75	1.74	0.829	0.915	0.622	0.215	0.487	1.51	1.50	0.932	1.351	0.958	0.311	1.368
Aegis T#2	1.46	1.70	0.625	1.260	0.641	0.119	0.315	1.32	1.31	0.781	1.430	1.251	0.128	0.934
Aegis T#3	2.05	2.02	0.790	1.244	0.769	0.112	0.434	1.91	1.90	0.849	2.190	1.885	0.187	0.941
Aegis T#4	1.30	1.49	0.794	1.141	0.383	0.254	0.425	1.30	1.29	1.204	2.740	-	0.317	1.180
Aegis T#5	2.09	2.21	0.691	1.065	1.370	0.140	0.563	1.69	1.68	0.881	1.647	1.847	0.281	0.974

Figures 10 and 11 illustrate the different failure modes recorded by sensors located at the peak of the TrusSteel truss's top chord and at the midpoint of the Aegis truss's bottom chord, respectively, for all single truss tests. Although these displacement sensors are recording data at different locations, we expected the data received from each to be very similar due to them being located the same distance along the length of the truss.

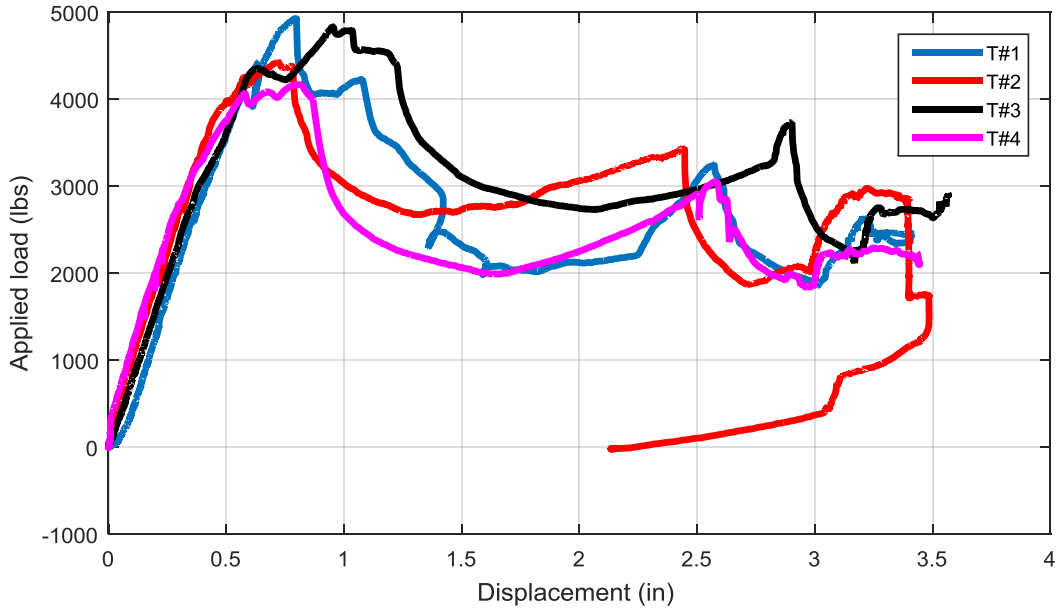

Figure 10: TrusSteel Testing summary of midpoint displacement sensor at top chord of trusses for all tests

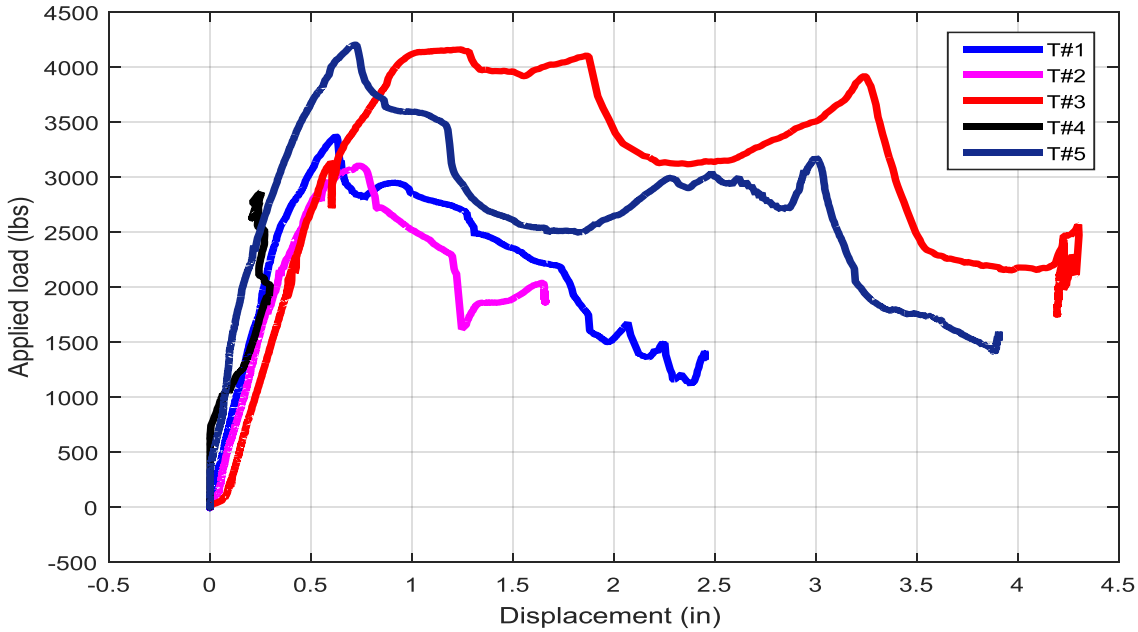

Figure 11: Aegis Testing summary of midpoint displacement sensor at bottom chord of trusses for all tests

Truss System Test Results

This research is investigating the system reliability of the trusses as well as their relationship between the components reliability. The failure sequences, load re-distribution mechanisms, and the load vs. deflection responses at various stages are being studied. For these truss system tests, more components were added to the test such as the corrugated b-decking to gather data on how the trusses will act in tandem with other trusses and connections. For each truss system tested, displacement sensors recorded the different movements at certain locations on the trusses. The locations are depicted in Figure 5, but essentially a sensor was located at both the peak and the middle of the bottom chord for the system. In addition to these two sensors, a sensor was located underneath each of the two loading points connected to the corrugated b-decking, and the fifth was located on the front of the truss to the top chord component to measure out-of-plane displacement.

Figures 12 and 13 illustrates the failure sequences of components, distributions of capacities at various stages in the failure process, and the system effects on capacity and ductility as well as illustrates a specific failure sequence and the load re-distribution mode that was observed on the system with two 23-feet long CFS TrusSteel profile and corrugated b-decking and CFS Aegis profile with corrugated b-decking respectively.

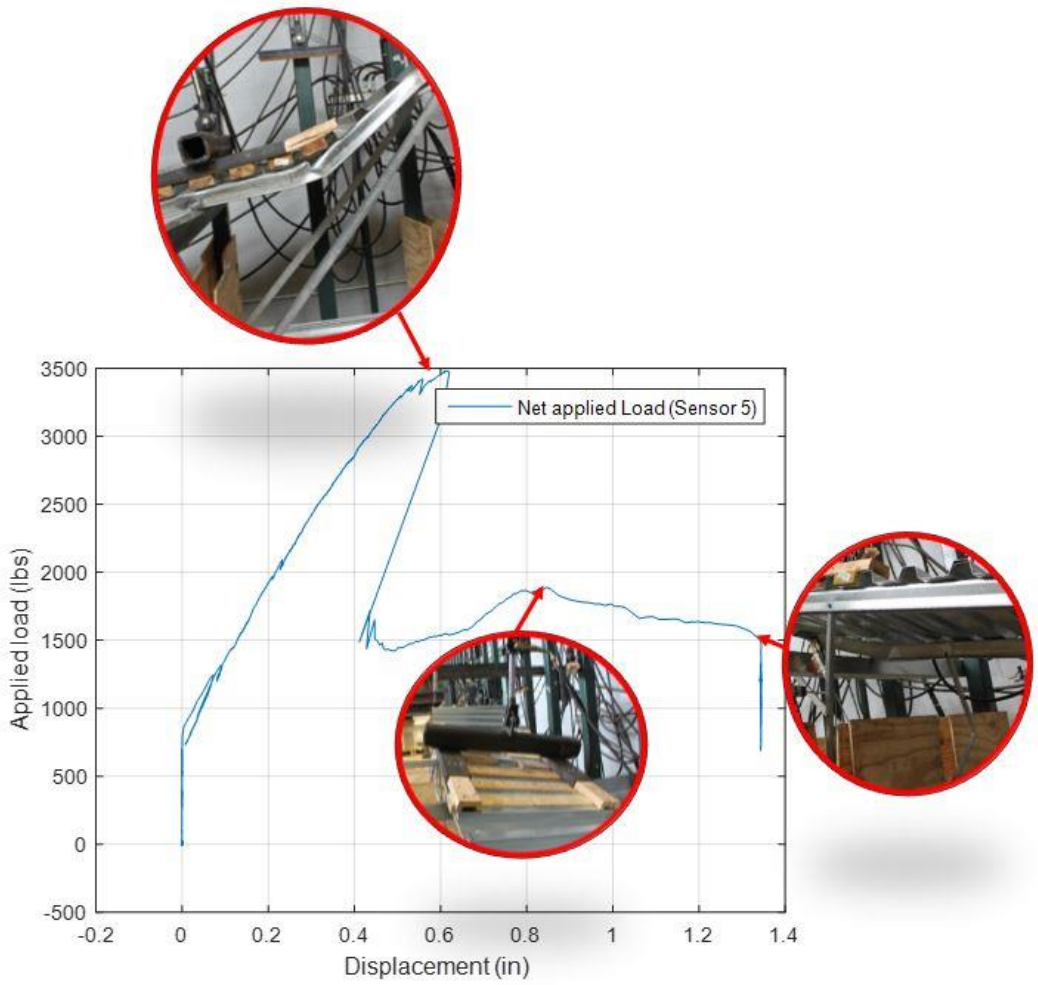

Figure 12: TrusSteel System Test Sensor located at the peak of the system with failure sequences and actual photos depicting the system failures

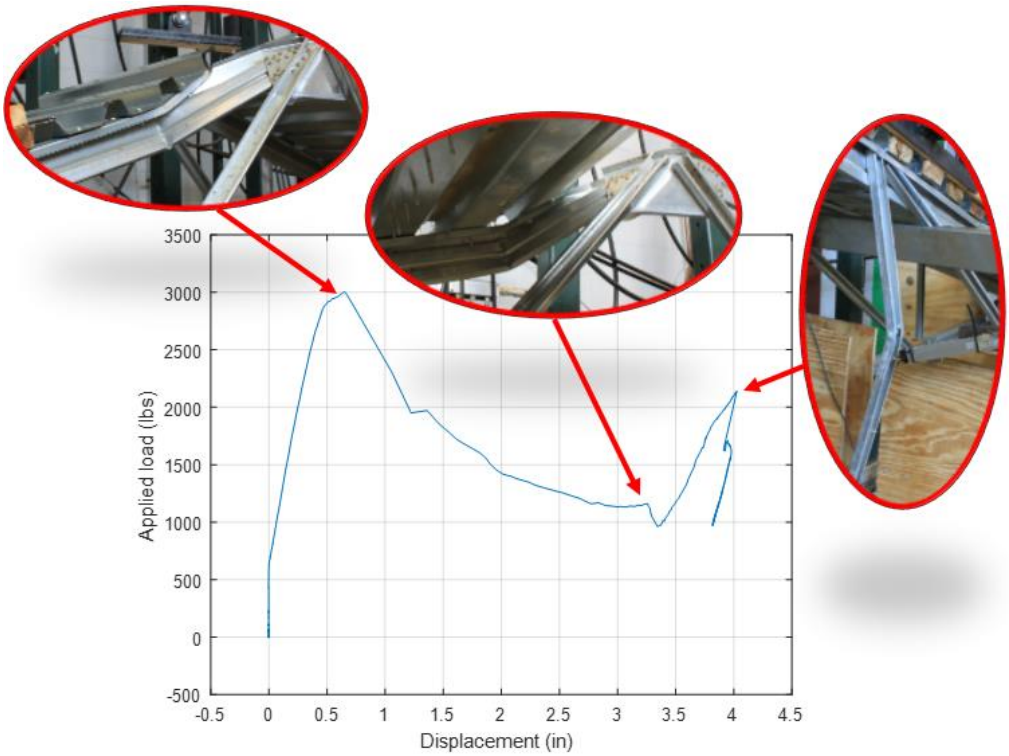

Figure 13: Aegis System Test Sensor located at the peak of the system with failure sequences and actual photos depicting the system failures

Table 5 lists the observed failure mode sequence for all truss system tests. Table 6 provides the peak loads and associated displacements for all truss system tests.

Table 5: Observed Failure Model for Truss System Tests

Truss Label	Failure Mode for 1st Peak	Failure Mode for 2nd Peak
TrusSteel Configuration	Top chord failures	Web member failures
Aegis Configuration	Top chord failures	Web member failures

Table 6: Test Results for Truss System Tests

Truss Label	1st Peak Load		Deflection @ 1st Peak				2nd Peak Load		Deflection @ 2nd Peak			
	Load Cell #1	Load Cell #2	Sensor #1	Sensor #2	Sensor #3	Sensor #4	Load Cell #1	Load Cell #2	Sensor #1	Sensor #2	Sensor #3	Sensor #4
TrusSteel T#1	1.57k	1.84k	0.445 (in)	0.036 (in)	1.252 (in)	0.875 (in)	0.867 k	0.983 k	1.616 (in)	0.037 (in)	3.215 (in)	1.463 (in)
TrusSteel T#2	1.6k	1.88k	1.376 (in)	0.005 (in)	1.093 (in)	0.614 (in)	0.895 k	1.015 k	1.601 (in)	0.006 (in)	2.285 (in)	1.347 (in)
TrusSteel T#3	1.59k	1.87k	0.836 (in)	0.041 (in)	1.064 (in)	0.582 (in)	1.17k	1.33k	1.414 (in)	0.041 (in)	1.224 (in)	0.908 (in)
Aegis T#1	1.51k	1.5k	-	0.002 (in)	-	0.649 (in)	1.15k	1.147 k	-	0.003 (in)	-	4.03 (in)
Aegis T#2	1.46k	1.45k	0.692 (in)	0.001 (in)	0.807 (in)	0.465 (in)	0.577 k	0.573 k	1.047 (in)	0.003 (in)	1.477 (in)	3.291 (in)
Aegis T#3	1.43k	1.42k	0.665 (in)	0.002 (in)	0.935 (in)	0.537 (in)	0.562 k	0.558 k	1.046 (in)	0.003 (in)	1.706 (in)	3.363 (in)

For all the system tests, it is important to note that only two load cells were used to measure the loads being applied to the system. However, four supports were used in total, so all peak loads are estimated to be about double what is shown in Table 6.

Conclusions

In summary, this project thus far has produced valuable data from both single and system truss tests using both truss configurations to aid in understanding the correlation between member reliability and system reliability. From these results, it strengthens our theory about this system reliability topic, which says that these trusses have component reliability failures in their chord and web members but when introduced into a system that can be thought of as a single component such as a truss with many webs and a top and bottom chord, it becomes increasingly clear that this system reliability is greater than any individual component reliability. From the single truss test results, it can be determined that each truss on its own will have approximately three failure sequences. However, from the data we have on the system truss tests with corrugated b-decking,

the data suggests that there will be at least two failure sequences but with some tests reaching up to three sequences as well. The next step of the research is to move forward with the finite element modeling and analysis of the truss configurations and to replicate virtually the results from our actual tests. The finite element model will be analyzed with a much greater precision and will ultimately aid in the calculations for predicting the failure loads for these truss configurations. By the same token, with the results that's already been produced from the tests, it can be said that progress has been made and moved us that much closer to a solution to system reliability in structural design. Therefore, for the next steps, perhaps methods can be developed for treating the structural system as an assembly of structural subsystems rather than an assembly of individual structural components. For example, a possibility may be the development of subsystem 'super-elements' that can be used to develop reduced degree-of-freedoms representations of the entire building.

Acknowledgements

This research was supported by the American Iron and Steel Institute. We would like to thank our colleagues from the University of Virginia Tech who provided insight and expertise that significantly assisted this research, although they may not agree with all the conclusions of this paper.

We thank Cris Moen, Ph.D., P.E., F.SEI for assistance with the introductory process and recommendations on procedures throughout the testing process and for his comments that helped mold this manuscript.

We would also like to show our momentous gratitude to the students working inside the University of North Texas Cold-formed Steel Research Lab that worked tirelessly to construct the truss testing setup and truss frames as well as the truss system tests. I am immensely grateful to Dr. Cheng Yu, PhD, who acted as the advising professor over this project, who offered his wisdom throughout the entire process, one of the few that reviewed this paper and offered comments on earlier versions of this manuscript and is seeing this project through till its final steps. With however, any errors are my own and should not tarnish the reputations of these esteemed persons.

References

Alireza, D., Houman, O. (2011).” A non-adapted sparse approximation of PDEs with stochastic inputs” J. Comput. Phys., 230 (8) (2011), pp. 3015–3034.

Arwade, M., Moradi, A. L. (2010) “Variance decomposition and global sensitivity for structural systems”. Eng. Structs., 32 (1) (2010), pp. 1–10.

Frangopol, D.M., Liu, M. (2007). “Maintenance and Management of Civil Infrastructure Based on Condition, Safety, Optimization and Life-Cycle Cost”. Struct Infr. Eng. 3 (1) (2007), pp. 29–41.

Landolfo R., Fiorino L., Della C. G. (2006). “Seismic behavior of sheathed cold-formed structures: physical tests.” J. Struct. Eng. 132(4) (2006); pp. 570-581.

Melchers R.E. (1987). “Structural Reliability Analysis and Prediction”, Ellis, Horwood Ltd, Chichester, England.

Nowak, A.S., Collins, K.R. (2000). “Reliability of structures.”, McGraw Hill, Boston, USA.

Rashedi, M.R., Moses, F. (1988) “Identification of failure modes in system reliability”. J. Struct. Eng. ASCE, 114(20 (1988), pp 292-313.

Serrette, R.L., Encalada, J., Juadines, M., Nguyen, H., (1997). “Static racking behavior of plywood, OSB, gypsum, and fiberboard walls with metal framing”. J. Struct. Eng. ASCE, 123 (8) (1997), pp. 1079–1086.

Sobol, I.M., (2001). “Global sensitivity indices for nonlinear mathematical models and their Monte Carlo estimates”. Math. Comp. Sim., 55 (2001), pp. 271–280.

Xiao, Q., Mahadevan, S., (1994), “Second-order upper bounds on probability of intersection of failure events”. J. Eng. Mech. 77 (1994), pp. 725-734.

Appendices

Cross sections for both configuration's top chords, bottom chords, and web members:

TrusSteel Top and bottom chord

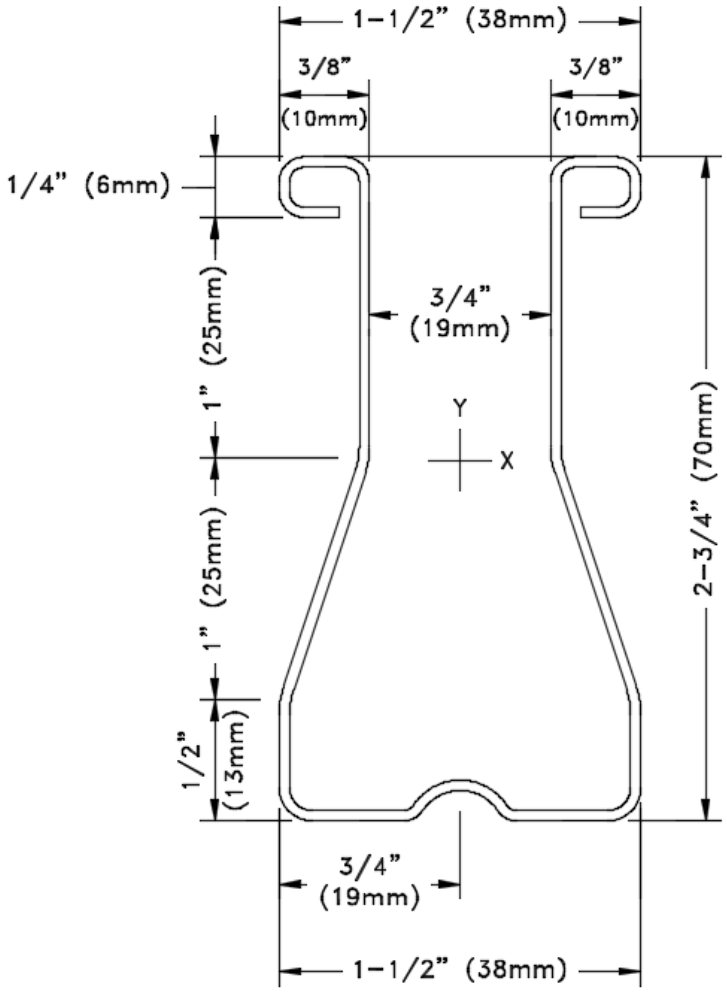

TSC2.75

Design thickness	0.0346 in.
F_y	55 ksi
F_u	65 ksi
Gauge	20

TrusSteel Web Members

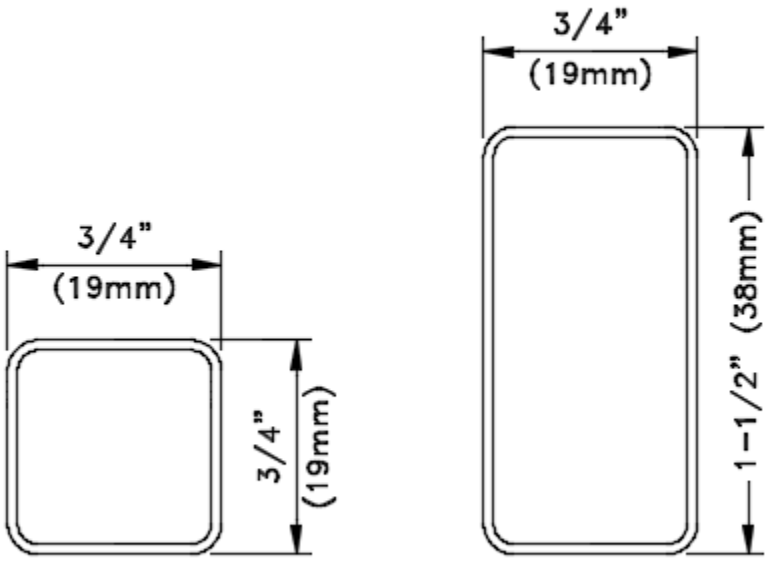

W.75x.75 W.75x1.5

Design thickness	**0.0350 in.**
F_y	**45 ksi**
F_u	**55 ksi**
Gauge	**20**

Aegis Top chord

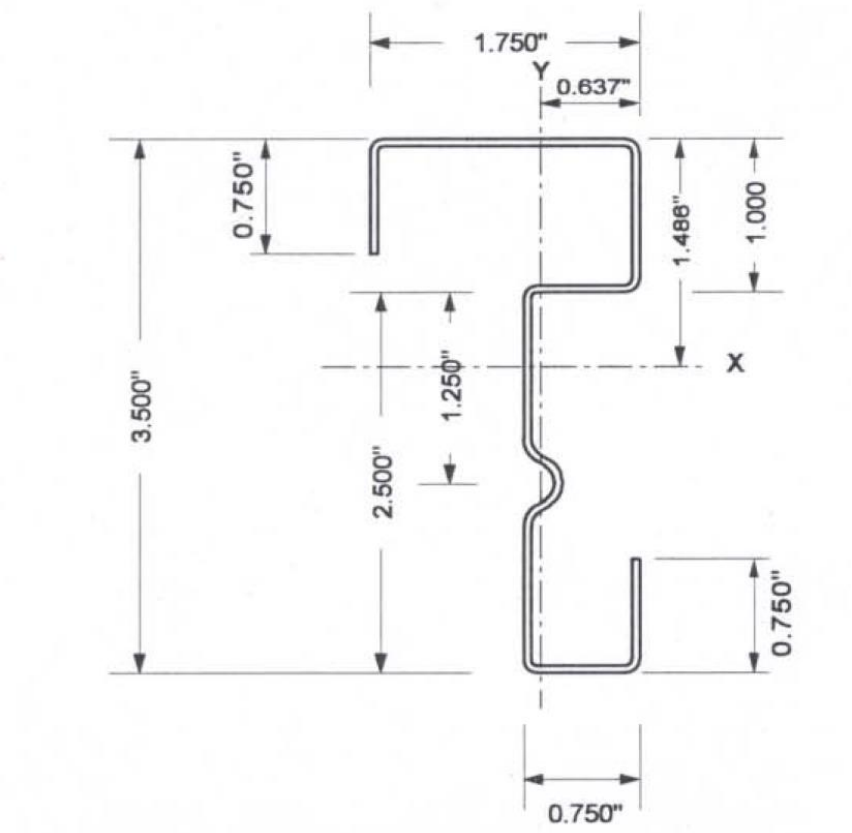

35USC035 50 - 3.5" x 1.75" 35 mil 50 ksi

Aegis Bottom chord

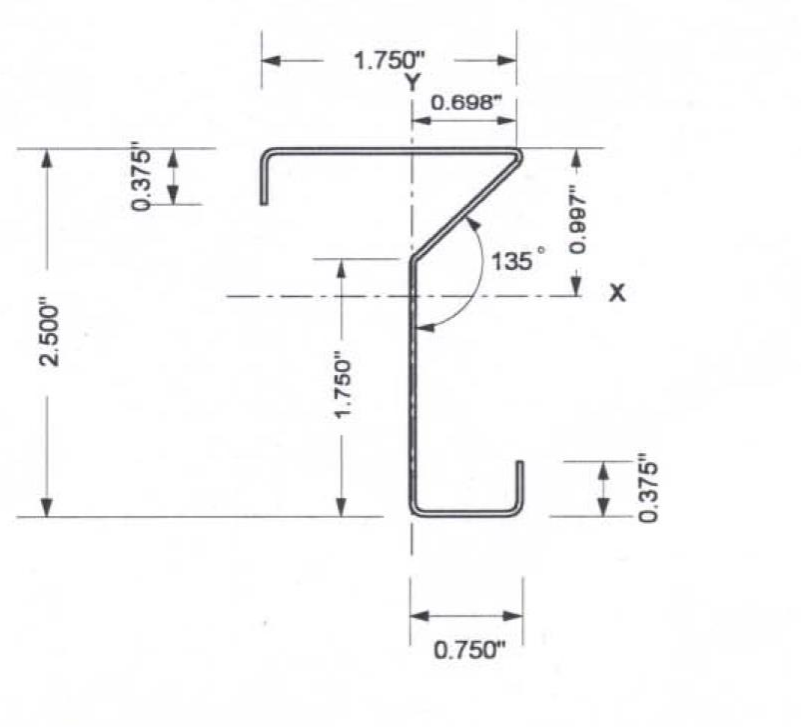

25USC035 50 - 2.5" x 1.75" 35 mil 50 ksi

Aegis Web members

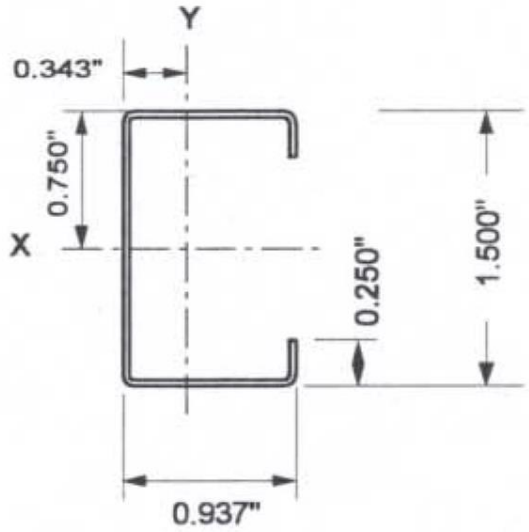

15USW035 50 - 1.5" x 0.937" 35 mil 50 ksi

American Iron and Steel Institute

25 Massachusetts Avenue, NW
Suite 800
Washington, DC 20001

www.steel.org

Research Report RP 17-1